

Non-Coherent Detection for Two-Way AF Cooperative Communications in Fast Rayleigh Fading Channels

Jian Tian, *Student Member, IEEE*, Qi Zhang, and Fengqi Yu

Abstract—Two-way cooperative communications are considered to improve the throughput of conventional one-way cooperative communications. For fast Rayleigh fading channels, we propose optimal and suboptimal non-coherent detectors for on-off keying (OOK) and frequency-shift keying (FSK) modulated two-way amplify-and-forward (AF) cooperative communications in this paper. In the proposed system, the relaying node combines the received signals from two nodes, amplifies them and retransmits the conjugate of the combined and amplified signals to the above-mentioned nodes. At the receivers of above-mentioned nodes, the optimal non-coherent detection is employed which is based on maximum likelihood rule. Since it involves integration operation, the optimal detector is simplified to a suboptimal detector which omits the real component of the relayed signal over the frequency which includes interference. The simulation results have shown that compared with the optimal detector, the proposed suboptimal detector reduces the receiver complexity at the expense of acceptable performance degradation. Furthermore, we have analytically studied the bit-error-rate performance upper and lower bounds of proposed non-coherent FSK modulated two-way AF cooperative communications.

Index Terms—Non-coherent detection, cooperative communication, amplify-and-forward (AF), two-way, Rayleigh fading.

I. INTRODUCTION

COOPERATIVE communications, which can provide extra spatial diversity for conventional single antenna transceivers to combat fading in wireless communication networks, have received more and more attentions [1]-[9]. In cooperative communications, the cooperative nodes relay the signals according to different relaying protocols, such as amplify-and-forward (AF), decode-and-forward (DF), and compress-and-forward (CF) [2]-[4]. Among them, AF protocol is widely employed in the situations where the relaying nodes have limited ability of signal processing.

The coherent detection for AF cooperative communications, studied in [5], requires perfect channel state information (CSI)

Paper approved by M.-S. Alouini, the Editor for Modulation and Diversity Systems of the IEEE Communications Society. Manuscript received August 19, 2009; revised April 15, 2010, December 16, 2010, and March 30, 2011.

This work was partially supported by the National S&T Key Project in China, under Grant No. 2009ZX03006-001-01, and by the Shenzhen Outstanding Youth Fund, under Grant No. JC201005270349A. This work was presented in part at the IEEE International Conference on Communications (ICC), Kyoto, Japan, June 2011.

The authors are with the Center for Integrated Electronics, Shenzhen Institutes of Advanced Technology, Chinese Academy of Sciences and The Chinese University of Hong Kong, 518055, P. R. China. J. Tian is also with the Institute of Microelectronics and Graduate School of the Chinese Academy of Sciences (e-mail: {jian.tian, qi.zhang, fq.yu}@siat.ac.cn).

Digital Object Identifier 10.1109/TCOMM.2011.080111.090491

known at the destination. To obtain CSI, we should transmit extra pilot symbols and estimate the wireless channels, which reduces the network throughput and increases the system complexity. Especially when the wireless channels vary rapidly, the coherent detection at the destination is almost impossible.

When coherent detection is impossible, non-coherent (de)modulations have been proposed in [6]-[9]. In [6], Annavajjala et al proposed optimal non-coherent detectors for on-off keying (OOK) and binary frequency-shift keying (FSK) modulated AF cooperative communications in a Rayleigh fading environment. However, the proposed optimal detectors are not in closed form and involve numerical integration, which makes the receiver have very high complexity. In [7], Zhu et al developed the suboptimal detectors as a low complexity counterpart for the above-mentioned optimal detectors by employing Jensen's inequality. Simulation results have shown that the suboptimal detectors are able to approach the performance of optimal detectors when the signal-to-noise-ratio (SNR) is high.

The work in [6]-[9] considers one-way cooperative communications. To improve the transmission efficiency and increase the network throughput, two-way cooperative communications employing network coding have been studied extensively [10]-[19]. The idea of two-way cooperative communications is that considering two nodes need to exchange information with each other, the third node cooperatively relays the combination of exchanged information symbols from both nodes by "XOR" operation [12] or other means [13]-[16] after receiving them. By employing these methods, the cooperative communications between the three nodes require less time slots.

The above-mentioned two-way cooperative communications consider coherent (de)modulations by assuming the channels are static or slow fading. However, for fast fading channels, above-mentioned schemes cannot be applied, especially for AF cooperative communications. In this paper, we propose optimal non-coherent detection for two-way OOK and M -ary FSK modulated AF cooperative communications in fast Rayleigh fading channels. In non-coherent two-way AF cooperative communications, how to combine the exchanged information symbols from two source nodes is a problem. In this paper, we propose simple addition, amplification, conjugate and retransmission operations on the received exchanged symbols from two source nodes. The proposed signal combination method facilitates the signal detection at the destination. Without channel state information (CSI), we derive

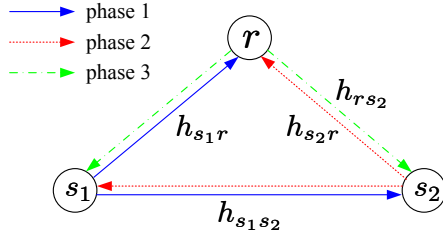


Fig. 1. System model for two-way cooperative communications.

the non-coherent optimal detectors for two-way AF cooperative communications. Since the optimal detectors involve integration operation, we derive a suboptimal detector without integration. Simulation results will be provided to show that the suboptimal detector is able to approach the bit-error-rate (BER) performance of the optimal detector. Furthermore, we analytically study the BER performance upper and lower bounds of proposed two-way M -ary FSK modulated AF cooperative communications.

The rest of this paper is organized as follows: Section II describes the system model of two-way AF cooperative communication network. We derive the non-coherent optimal and suboptimal detectors in Section III and Section IV, respectively. In Section V, we derive the optimal detector when the partial CSI is known. In Section VI, the BER performance upper and lower bounds of proposed two-way FSK modulated AF cooperative communications are studied. Computer simulated results are presented and discussed in Section VII. Finally, conclusions are given in Section VIII.

II. SYSTEM MODEL

In flat Rayleigh fading channels, we consider a three-node two-way wireless cooperative communication network where nodes s_1 and s_2 communicate with each other with the assistance of node r , as illustrated in Fig. 1. In this two-way cooperative communication network, each node works in half-duplex mode. This is because each node cannot transmit and receive signals simultaneously on the same frequency band. Thus, the exchange of information symbols between nodes s_1 and s_2 is divided into three phases. In the first and second phases, nodes s_1 and s_2 broadcast their signals, respectively. In the third phase, node r broadcasts the combination of the received signals from nodes s_1 and s_2 .

The nodes s_1 and s_2 employ an on-off keying (OOK) or M -ary frequency shift keying (FSK) modulation to transmit signals. Denote the modulated signals at nodes s_1 and s_2 as vectors \mathbf{x}_{s_1} and \mathbf{x}_{s_2} with length M , respectively. The vectors $\mathbf{x}_{s_1}, \mathbf{x}_{s_2} \in \Theta$,

$$\Theta = \begin{cases} \{\sqrt{2E_s}, 0\}; & \text{OOK} \\ \{\mathbf{x}_m, m = 2, 3, \dots, M\}; & M\text{-ary FSK} \end{cases} \quad (1)$$

where E_s is the transmission power per symbol and

$$\mathbf{x}_m = \left[\underbrace{0, \dots, 0}_{m-1}, \sqrt{E_s}, \underbrace{0, \dots, 0}_{M-m} \right]^\dagger \quad (2)$$

in which \dagger denotes the transpose and conjugate operation. Thus OOK can be seemed as a special case of M -ary FSK where

$M = 1$. Without loss of generality, we only focus on the signals transmitted from the node s_1 to the node s_2 in this paper. The relationships between the transmitted and received signals at nodes r and s_2 are as follows

$$\mathbf{y}_{s_1s_2} = h_{s_1s_2}\mathbf{x}_{s_1} + \mathbf{n}_{s_1s_2}, \quad (3)$$

$$\mathbf{y}_{s_1r} = h_{s_1r}\mathbf{x}_{s_1} + \mathbf{n}_{s_1r}, \quad (4)$$

$$\mathbf{y}_{s_2r} = h_{s_2r}\mathbf{x}_{s_2} + \mathbf{n}_{s_2r}, \quad (5)$$

$$\mathbf{y}_{rs_2} = A_r h_{rs_2} (\mathbf{y}_{s_1r} + \mathbf{y}_{s_2r})^* + \mathbf{n}_{rs_2} \quad (6)$$

where $*$ denotes the conjugate operation. In (3)-(6), the vector \mathbf{y}_{pq} with length M denotes the received signals at node q transmitted from node p , $p, q \in \{s_1, r, s_2\}$, whose m^{th} entry is the received signal over the m^{th} frequency; h_{pq} denotes the channel fading coefficient from node p to node q ; and the vector \mathbf{n}_{pq} with length M denotes the additive white Gaussian noise (AWGN) at node q when node p broadcasts signals, whose m^{th} entry is the AWGN over the m^{th} frequency. The channel fading coefficient h_{pq} is a circular symmetric complex Gaussian random variable (RV) with variance Ω_{pq} , where $\Omega_{pq} = \Omega_{qp}$. Same as the channel fading coefficient, the entry of the noise vector \mathbf{n}_{pq} is also circular symmetric complex Gaussian RV, whose variance is N_o . In (3)-(6), the fading coefficients $h_{s_1s_2}, h_{s_1r}, h_{s_2r}$ are mutually independent and $h_{s_1s_2}, h_{s_1r}, h_{rs_2}$ are also mutually independent. However, due to the channel symmetry, h_{s_2r} and h_{rs_2} are correlated RVs whose correlation coefficient is denoted as ρ . In this paper, we focus on fast fading channel. The instantaneous channel fading coefficients $\{h_{s_1s_2}, h_{s_1r}, h_{s_2r}, h_{rs_2}\}$ are assumed to be unknown at any node. Hence node s_2 has to employ non-coherent detection. In (6), A_r is the amplification factor which satisfies the long-term power constraint for ergodic channels

$$A_r^2 E \left[(\mathbf{y}_{s_1r} + \mathbf{y}_{s_2r})^\dagger (\mathbf{y}_{s_1r} + \mathbf{y}_{s_2r}) \right] = E_r \quad (7)$$

where $E[\bullet]$ denotes the expectation of $[\bullet]$ and E_r denotes the transmission power per symbol at node r . Thus,

$$A_r = \left(\frac{E_r}{E_s \Omega_{s_1r} + E_s \Omega_{s_2r} + 2MN_o} \right)^{\frac{1}{2}}. \quad (8)$$

It is worth noting that in (6), the relayed signal is actually conjugate version of the received signals at node r . In doing that, the complexity of the relaying nodes is increased a little whereas the complexity of the proposed detector is reduced significantly compared with the relaying without conjugate operation. This is because by conjugate operation, we can exploit the correlation of the channel coefficients h_{s_2r} and h_{rs_2} .

III. OPTIMAL DETECTOR UNDER MAXIMUM LIKELIHOOD RULE

We consider to employ maximum likelihood detection rule to detect the received signals at node s_2 . The estimated symbol transmitted from node s_1 is expressed as follows

$$\hat{\mathbf{x}}_{s_1} = \arg \max_{\mathbf{x}_{s_1} \in \Theta} P(\mathbf{y}_{s_1s_2}, \mathbf{y}_{rs_2} | \mathbf{x}_{s_1}, \mathbf{x}_{s_2}) \quad (9)$$

where $P(\mathbf{y}_{pq} | \mathbf{x}_p)$ is the conditional probability density function (PDF) of \mathbf{y}_{pq} given \mathbf{x}_p . Since the channels $h_{s_1s_2}, h_{s_1r}$,

and h_{rs_2} are mutually independent, the conditional PDF $p(\mathbf{y}_{s_1s_2}, \mathbf{y}_{rs_2} | \mathbf{x}_{s_1}, \mathbf{x}_{s_2})$ can be reduced to

$$P(\mathbf{y}_{s_1s_2}, \mathbf{y}_{rs_2} | \mathbf{x}_{s_1}, \mathbf{x}_{s_2}) = P(\mathbf{y}_{s_1s_2} | \mathbf{x}_{s_1})P(\mathbf{y}_{rs_2} | \mathbf{x}_{s_1}, \mathbf{x}_{s_2}). \quad (10)$$

In (9)-(10), $\mathbf{y}_{s_1s_2}$ is M -dimensional complex Gaussian distributed with mean vector $\mathbf{0}$ and covariance matrix

$$\Psi_{s_1s_2} = N_o \mathbf{I}_M + \Omega_{s_1s_2} \mathbf{x}_{s_1} \mathbf{x}_{s_1}^\dagger \quad (11)$$

where \mathbf{I}_M is an $M \times M$ identity matrix. Thus, the conditional PDF of $\mathbf{y}_{s_1s_2}$ on \mathbf{x}_{s_1} is

$$P(\mathbf{y}_{s_1s_2} | \mathbf{x}_{s_1}) = \frac{1}{\pi^M \det(\Psi_{s_1s_2})} \exp(-\mathbf{y}_{s_1s_2}^\dagger \Psi_{s_1s_2}^{-1} \mathbf{y}_{s_1s_2}) \quad (12)$$

where $\det(\bullet)$ denotes the determinant of (\bullet) . The computation of $P(\mathbf{y}_{rs_2} | \mathbf{x}_{s_1}, \mathbf{x}_{s_2})$ is not straightforward because the transmission of \mathbf{x}_{s_2} from node s_2 affects the relaying signal. From (3)-(6), we have

$$\mathbf{y}_{rs_2} = A_r h_{rs_2} (h_{s_1r} \mathbf{x}_{s_1} + h_{s_2r} \mathbf{x}_{s_2} + \mathbf{n}_{s_1r} + \mathbf{n}_{s_2r})^* + \mathbf{n}_{rs_2}. \quad (13)$$

Since h_{rs_2} and h_{s_2r} are correlated with the correlation coefficient ρ , we can express h_{s_2r} as follows

$$h_{s_2r} = \rho h_{rs_2} + \eta \quad (14)$$

where η is a circular symmetric complex Gaussian RV with zero mean and variance $(1 - \rho^2) \Omega_{rs_2}$ and η is uncorrelated with h_{rs_2} . Therefore, we can rewrite (13) as follows

$$\mathbf{y}_{rs_2} = A_r h_{rs_2} (h_{s_1r} \mathbf{x}_{s_1} + \rho h_{rs_2} \mathbf{x}_{s_2})^* + A_r h_{rs_2} (\eta \mathbf{x}_{s_2} + \mathbf{n}_{s_1r} + \mathbf{n}_{s_2r})^* + \mathbf{n}_{rs_2}. \quad (15)$$

Given \mathbf{x}_{s_1} , \mathbf{x}_{s_2} , h_{s_1r} and h_{rs_2} , \mathbf{y}_{rs_2} is M -dimensional complex Gaussian distributed with mean vector

$$\xi = A_r h_{rs_2} (h_{s_1r} \mathbf{x}_{s_1} + \rho h_{rs_2} \mathbf{x}_{s_2})^* \quad (16)$$

and covariance matrix

$$\Psi_\xi = A_r^2 |h_{rs_2}|^2 (1 - \rho^2) \Omega_{rs_2} \mathbf{x}_{s_2} \mathbf{x}_{s_2}^\dagger + N_o (1 + 2A_r^2 |h_{rs_2}|^2) \mathbf{I}_M. \quad (17)$$

The conditional PDF of \mathbf{y}_{rs_2} on \mathbf{x}_{s_1} , \mathbf{x}_{s_2} , h_{s_1r} and h_{rs_2} is

$$P(\mathbf{y}_{rs_2} | \mathbf{x}_{s_1}, \mathbf{x}_{s_2}, h_{s_1r}, h_{rs_2}) = \frac{1}{\pi^M \det(\Psi_\xi)} \exp[-(\mathbf{y}_{rs_2} - \xi)^\dagger \Psi_\xi^{-1} (\mathbf{y}_{rs_2} - \xi)]. \quad (18)$$

To derive the conditional PDF $P(\mathbf{y}_{rs_2} | \mathbf{x}_{s_1}, \mathbf{x}_{s_2})$, we need the following lemma which is from [6]

Lemma 1 : If Z is circular symmetric complex Gaussian random variable with the mean m_z and variance σ_z^2 , then the expected value of $\exp(-|Z|^2)$ is

$$\mathbb{E}[\exp(-|Z|^2)] = \frac{1}{1 + \sigma_z^2} \exp\left(-\frac{|m_z|^2}{1 + \sigma_z^2}\right). \quad (19)$$

With Lemma 1, the conditional PDF $P(\mathbf{y}_{rs_2} | \mathbf{x}_{s_1}, \mathbf{x}_{s_2}, h_{rs_2})$ is obtained by taking expectation over h_{s_1r} . Given h_{rs_2} , \mathbf{y}_{rs_2} is M -dimensional complex Gaussian distributed with mean vector

$$\bar{\mathbf{y}}_{rs_2} = \rho A_r |h_{rs_2}|^2 \mathbf{x}_{s_2} \quad (20)$$

and covariance matrix

$$\Psi_{rs_2} = \Psi_\xi + A_r^2 |h_{rs_2}|^2 \Omega_{s_1r} \mathbf{x}_{s_1} \mathbf{x}_{s_1}^\dagger. \quad (21)$$

The conditional PDF of \mathbf{y}_{rs_2} on \mathbf{x}_{s_1} , \mathbf{x}_{s_2} and h_{rs_2} is

$$P(\mathbf{y}_{rs_2} | \mathbf{x}_{s_1}, \mathbf{x}_{s_2}, h_{rs_2}) = \frac{1}{\pi^M \det(\Psi_{rs_2})} \exp\left[-(\mathbf{y}_{rs_2} - \bar{\mathbf{y}}_{rs_2})^\dagger \Psi_{rs_2}^{-1} (\mathbf{y}_{rs_2} - \bar{\mathbf{y}}_{rs_2})\right]. \quad (22)$$

Taking the expectation of (22) over $|h_{rs_2}|^2$, we obtain the conditional PDF $P(\mathbf{y}_{rs_2} | \mathbf{x}_{s_1}, \mathbf{x}_{s_2})$

$$P(\mathbf{y}_{rs_2} | \mathbf{x}_{s_1}, \mathbf{x}_{s_2}) = \int_0^\infty \frac{\pi^{-M}}{\Omega_{rs_2} \det(\Psi_z)} \exp\left[-\frac{z}{\Omega_{rs_2}} - (\mathbf{y}_{rs_2} - z \rho A_r \mathbf{x}_{s_2})^\dagger \Psi_z^{-1} (\mathbf{y}_{rs_2} - z \rho A_r \mathbf{x}_{s_2})\right] dz \quad (23)$$

where

$$\Psi_z = z A_r^2 (\Omega_{rs_2} (1 - \rho^2) \mathbf{x}_{s_2} \mathbf{x}_{s_2}^\dagger + \Omega_{s_1r} \mathbf{x}_{s_1} \mathbf{x}_{s_1}^\dagger) + N_o (1 + 2z A_r^2) \mathbf{I}_M. \quad (24)$$

To our best knowledge, the closed-form expressions of (23) does not exist in the literature. In Section VII, we calculate (23) numerically to obtain the simulation results of proposed optimal receivers.

IV. SUBOPTIMAL DETECTOR

The optimal detector under maximum likelihood rule involves integration operation which is complicated. In this section, we will derive suboptimal detector without integration operation. The proposed suboptimal detector reduces the system complexity at the expense of slight performance degradation.

We rewrite the expression (15) as follows

$$\mathbf{y}_{rs_2} - \mathbf{n}_{rs_2} = A_r h_{rs_2} (h_{s_1r} \mathbf{x}_{s_1} + \rho h_{rs_2} \mathbf{x}_{s_2} + \eta \mathbf{x}_{s_2} + \mathbf{n}_{s_1r} + \mathbf{n}_{s_2r})^*. \quad (25)$$

In (25), $\mathbf{y}_{rs_2} - \mathbf{n}_{rs_2}$ is a vector with length M whose entry is the product of two complex Gaussian RVs. Without loss of generality, we assume that in vector \mathbf{x}_{s_2} , the l^{th} entry is nonzero. The proposed suboptimal detector only employs y_{l/rs_2} and the imaginary component of $y_{rs_2,l}$ for symbol detection, where $\mathbf{z}_{l/p}$ denotes the vector \mathbf{z}_p without the l^{th} entry and $z_{p,l}$ denotes the l^{th} entry of \mathbf{z}_p . Thus, the estimated symbol transmitted from node s_1 by employing the suboptimal detection is expressed as follows

$$\hat{\mathbf{x}}_{s_1} = \arg \max_{\mathbf{x}_{s_1} \in \Theta} P(\text{Im}(y_{rs_2,l}) | \mathbf{x}_{s_1}, \mathbf{x}_{s_2}) \cdot P(y_{l/rs_2} | \mathbf{x}_{s_1}, \mathbf{x}_{s_2}) \cdot P(\mathbf{y}_{s_1s_2} | \mathbf{x}_{s_1}). \quad (26)$$

The proposed suboptimal detector discards the real component of $y_{rs_2,l}$ because the real component contains the interference $\rho A_r |h_{rs_2}|^2 \mathbf{x}_{s_2}$, which is an exponential distributed RV. Thus, we propose to derive the suboptimal detector without considering the real component of $y_{rs_2,l}$.

The imaginary component of $y_{rs_2,l} - n_{rs_2,l}$, denoted as

$\text{Im}(y_{rs_2,l} - n_{rs_2,l})$, is

$$\begin{aligned} & \text{Im}(y_{rs_2,l} - n_{rs_2,l}) \\ &= A_r \text{Im} \left[h_{rs_2} (h_{s_1r} x_{s_1,l} + \eta x_{s_2,l} + n_{s_1r,l} + n_{s_2r,l})^* \right] \end{aligned} \quad (27)$$

whose entry is the inner product of two independent zero mean Gaussian vectors with length of two. The conditional PDF $P[\text{Im}(y_{rs_2,l} - n_{rs_2,l}) | \mathbf{x}_{s_1}, \mathbf{x}_{s_2}]$ is [20]

$$\begin{aligned} & P[\text{Im}(y_{rs_2,l} - n_{rs_2,l}) | \mathbf{x}_{s_1}, \mathbf{x}_{s_2}] \\ &= \frac{1}{\sqrt{\psi_l}} \exp \left[-2\psi_l^{-\frac{1}{2}} |\text{Im}(y_{rs_2,l} - n_{rs_2,l})| \right] \end{aligned} \quad (28)$$

where

$$\psi_l = A_r^2 \Omega_{rs_2} \left[A_r^2 \Omega_{s_1r} x_{s_1,l}^2 + (1 - \rho^2) \Omega_{rs_2} x_{s_2,l}^2 + 2N_o \right]. \quad (29)$$

Thus the conditional PDF $P[\text{Im}(y_{rs_2,l} - n_{rs_2,l}) | \mathbf{x}_{s_1}, \mathbf{x}_{s_2}]$ can be achieved by taking expectation of expression (28) over $n_{rs_2,l}$. Unfortunately, to best of our knowledge, there is no closed form expression available for above-mentioned expectation. As an alternative, we will employ the Jensen's inequality to obtain the lower bound of the expectation. By applying Jensen's inequality, we have

$$\begin{aligned} & P[\text{Im}(y_{rs_2,l}) | \mathbf{x}_{s_1}, \mathbf{x}_{s_2}] \\ & \geq \frac{1}{\sqrt{\psi_l}} \exp \left[-2\psi_l^{-\frac{1}{2}} \sqrt{\text{E}(\text{Im}(y_{rs_2,l} - n_{rs_2,l})^2)} \right] \\ & = \frac{1}{\sqrt{\psi_l}} \exp \left[-2\psi_l^{-\frac{1}{2}} \sqrt{\text{Im}^2(y_{rs_2,l}) + N_o/2} \right]. \end{aligned} \quad (30)$$

In (30), the Jensen's inequality is valid because $\exp(-\sqrt{x})$ is a convex function whose second-order derivative is greater than or equal to zero, i.e.

$$\frac{d^2}{dx^2} [\exp(-\sqrt{x})] = \frac{x^{-\frac{3}{2}}}{4} \exp(-\sqrt{x}) + \frac{1}{4x} \exp(-\sqrt{x}) \geq 0. \quad (31)$$

The expression of vector \mathbf{y}_{l/rs_2} is as follows

$$(\mathbf{y}_{l/rs_2} - \mathbf{n}_{l/rs_2}) = A_r h_{rs_2} (h_{s_1r} \mathbf{x}_{l/s_1} + \mathbf{n}_{l/s_1r} + \mathbf{n}_{l/s_2r})^* \quad (32)$$

whose entry is the product of two independent zero mean complex Gaussian RVs. By applying Jensen's inequality as in [7], we have

$$P(\mathbf{y}_{l/rs_2} | \mathbf{x}_{s_1}, \mathbf{x}_{s_2}) \approx \prod_{i=1, i \neq l}^M \frac{2}{\pi \psi_i} K_0 \left(2\psi_i^{-\frac{1}{2}} \sqrt{|y_{rs_2,i}|^2 + N_o} \right) \quad (33)$$

where $K_0(\bullet)$ is the zero-order modified Bessel function of the second kind and

$$\psi_i = A_r^2 \Omega_{rs_2} (\Omega_{s_1r} x_{s_1,i}^2 + 2N_o), \quad i \neq l. \quad (34)$$

The above suboptimal detector is obtained without considering the real component of $y_{rs_2,l}$. It is worth noting that when $\rho = 0$, the interference $\rho A_r |h_{rs_2}|^2 \mathbf{x}_{s_2}$ does not exist. Under this situation, the suboptimal detector still employs (9)-(10) for symbol detection with $P(\mathbf{y}_{rs_2} | \mathbf{x}_{s_1}, \mathbf{x}_{s_2})$ is replaced by

$$P(\mathbf{y}_{rs_2} | \mathbf{x}_{s_1}, \mathbf{x}_{s_2}) \approx \prod_{i=1}^M \frac{2}{\pi \psi_i} K_0 \left(2\psi_i^{-\frac{1}{2}} \sqrt{|y_{rs_2,i}|^2 + N_o} \right). \quad (35)$$

V. OPTIMAL DETECTOR WITH PARTIAL CSI

In the above two-way AF cooperative communications, we assume that the nodes have no channel state information (CSI). This assumption is valid when the whole communication network undergoes fast fading. In practical systems, another situation that one source node, s_1 or s_2 , is moving at a high speed, the other one and node r are static may be common. Without loss of generality, we assume that node s_1 is moving. Under this situation, the channels from node s_2 to node s_1 and from node r to node s_1 undergo fast fading whereas the channel from node r to node s_2 is quasi-static or undergoes slow fading. Thus, the detector at node s_1 has to employ the optimal or suboptimal schemes proposed in Sections III and IV for symbol detection whereas the node s_2 may exploit the CSI of h_{rs_2} to improve the system performance. When the detection at node s_2 is considered, the node r does not exploit the CSI of h_{s_2r} since it is assumed to have limited signal processing power and it just amplifies and forwards its received signals.

With the knowledge of h_{rs_2} , the optimal detector at the node s_2 is derived as follows. From (15), we obtain

$$\begin{aligned} \mathbf{y}_{rs_2} &= \rho A_r |h_{rs_2}|^2 \mathbf{x}_{s_2} \\ &+ A_r h_{rs_2} (h_{s_1r} \mathbf{x}_{s_1} + \eta \mathbf{x}_{s_2} + \mathbf{n}_{s_1r} + \mathbf{n}_{s_2r})^* + \mathbf{n}_{rs_2}. \end{aligned} \quad (36)$$

Given \mathbf{x}_{s_1} and \mathbf{x}_{s_2} , \mathbf{y}_{rs_2} is M -dimensional complex Gaussian distributed with mean vector

$$\xi_p = \rho A_r |h_{rs_2}|^2 \mathbf{x}_{s_2} \quad (37)$$

and covariance matrix

$$\begin{aligned} \Psi_p &= A_r^2 |h_{rs_2}|^2 [\Omega_{s_1r} \mathbf{x}_{s_1} \mathbf{x}_{s_1}^\dagger + (1 - \rho^2) \Omega_{rs_2} \mathbf{x}_{s_2} \mathbf{x}_{s_2}^\dagger + 2N_o \mathbf{I}_M] \\ &+ N_o \mathbf{I}_M. \end{aligned} \quad (38)$$

The conditional PDF of \mathbf{y}_{rs_2} on \mathbf{x}_{s_1} and \mathbf{x}_{s_2} is

$$\begin{aligned} P(\mathbf{y}_{rs_2} | \mathbf{x}_{s_1}, \mathbf{x}_{s_2}) &= \frac{1}{\pi^M \det(\Psi_p)} \\ &\exp \left[-(\mathbf{y}_{rs_2} - \xi_p)^\dagger \Psi_p^{-1} (\mathbf{y}_{rs_2} - \xi_p) \right]. \end{aligned} \quad (39)$$

Substitute (39) into (9)-(10), we obtain the estimated symbol transmitted from node s_1 for the optimal detector with partial CSI.

VI. BER PERFORMANCE UPPER AND LOWER BOUNDS

In this section, we will derive the bit-error-rate (BER) performance upper and lower bounds of the optimal non-coherent detector for M -ary FSK modulated two-way AF cooperative communications in Rayleigh fading channels.

A. BER Performance Lower Bound

Without loss of generality, we assume that $\mathbf{x}_{s_1} = \mathbf{x}_1$ and $\mathbf{x}_{s_2} = \mathbf{x}_l$. From (23), the optimal detector involves integration operation which causes the exact analytical BER performance is difficult to obtain. The integration operation in the optimal detector is due to the interference \mathbf{x}_{s_2} included in \mathbf{y}_{rs_2} which causes the expression for probability distribution of the real component of $y_{rs_2,l}$ to be very complicated. However, from Section V, we know that with the partial CSI h_{rs_2} , the

conditional PDF $P(\mathbf{y}_{rs_2} | \mathbf{x}_{s_1}, \mathbf{x}_{s_2})$ can be achieved in a close form thus the performance analysis for the optimal detector with partial CSI is possible. In this paper, we propose to derive the BER performance of optimal detector with partial CSI for two-way AF cooperative communications which is the lower bound of optimal detector without partial CSI.

From (9)-(10), the pairwise error probability of \mathbf{x}_1 erroneously detected as \mathbf{x}_k , $k \in \{2, 3, \dots, M\}$, is expressed as follows

$$P(\mathbf{x}_1 \rightarrow \mathbf{x}_k) = P(\lambda_{1k} < 0) \quad (40)$$

where

$$\lambda_{1k} = \log \frac{P(\mathbf{y}_{s_1 s_2} | \mathbf{x}_1) P(\mathbf{y}_{rs_2} | \mathbf{x}_1, \mathbf{x}_l)}{P(\mathbf{y}_{s_1 s_2} | \mathbf{x}_k) P(\mathbf{y}_{rs_2} | \mathbf{x}_k, \mathbf{x}_l)}. \quad (41)$$

After some mathematical manipulation, we obtain [21]

$$\lambda_{1k} = U_1 - U_k + V_1 - V_k \quad (42)$$

where U_m and V_m , $m \in \{1, 2, \dots, M\}$, are shown on the top of the next page, in which $m \in \{1, 2, \dots, M\}$,

$$\gamma = \frac{E_s}{N_o}, \quad (45)$$

$$\beta_1 = \frac{1}{1 + A_r^2 |h_{rs_2}|^2 (2 + \gamma(1 - \rho^2) \Omega_{rs_2})} - \frac{1}{1 + A_r^2 |h_{rs_2}|^2 (2 + \gamma \Omega_{s_1 r} + \gamma(1 - \rho^2) \Omega_{rs_2})}, \quad (46)$$

$$\beta_2 = \frac{1}{1 + 2A_r^2 |h_{rs_2}|^2} - \frac{1}{1 + A_r^2 |h_{rs_2}|^2 (2 + \gamma \Omega_{s_1 r})}. \quad (47)$$

In (43), regardless of $l = m$ or $l \neq m$, ξ_m is the sum of two weighted independent chi-square distributed RVs, whose PDF is [20]

$$P_{U_m}(z) = \frac{1}{W_1 - W_2} \left(\exp\left(-\frac{z}{W_1}\right) - \exp\left(-\frac{z}{W_2}\right) \right), \quad z \geq 0, W_1 \neq W_2 \quad (48)$$

where

$$W_1 = \begin{cases} \delta_{11} = \gamma \Omega_{s_1 s_2}; & m = 1 \\ \delta_{12} = \frac{\gamma \Omega_{s_1 s_2}}{1 + \gamma \Omega_{s_1 s_2}}; & m \neq 1 \end{cases} \quad (49)$$

and W_2 is shown on the top of the next page. Therefore, when $l = 1$, i.e. $\mathbf{x}_{s_1} = \mathbf{x}_{s_2}$, the conditional probability of correct detection is evaluated as follows

$$\begin{aligned} P(c | \mathbf{x}_{s_1} = \mathbf{x}_{s_2}, h_{rs_2}) &= P\left(\bigcap_{k=2}^M \lambda_{1k} > 0\right) \\ &= \int_0^\infty P_{\xi_{11}}(z_1) \cdot \left(\prod_{k=2}^M \int_0^{z_1 + \zeta_1 - \zeta_2} P_{\xi_{k2}}(z_k) dz_k \right) dz_1 \\ &= \int_0^\infty \frac{1}{\delta_{11} - \delta_{21}} \left(\exp\left(-\frac{z_1}{\delta_{11}}\right) - \exp\left(-\frac{z_1}{\delta_{21}}\right) \right) \\ &\quad \cdot \left[\int_0^{z_1 + \zeta_1 - \zeta_2} \frac{1}{\delta_{12} - \delta_{24}} \left(\exp\left(-\frac{z_2}{\delta_{12}}\right) - \exp\left(-\frac{z_2}{\delta_{24}}\right) \right) dz_2 \right]^{M-1} dz_1. \end{aligned} \quad (51)$$

Similarly, when $l \neq 1$, i.e. $\mathbf{x}_{s_1} \neq \mathbf{x}_{s_2}$, the conditional probability of correct detection is evaluated as follows

$$P(c | \mathbf{x}_{s_1} \neq \mathbf{x}_{s_2}, h_{rs_2}) = \int_0^\infty P_{\xi_{12}}(z_1) \cdot \int_0^{z_1 + \zeta_2 - \zeta_1} P_{\xi_{11}}(z_1) dz_1$$

$$\begin{aligned} &\cdot \left(\prod_{k=2, k \neq l}^M \int_0^{z_1} P_{\xi_{k2}}(z_k) dz_k \right) dz_1 \\ &= \int_0^\infty \frac{1}{\delta_{11} - \delta_{23}} \left(\exp\left(-\frac{z_1}{\delta_{11}}\right) - \exp\left(-\frac{z_1}{\delta_{23}}\right) \right) \\ &\quad \cdot \int_0^{z_1 + \zeta_2 - \zeta_1} \frac{1}{\delta_{12} - \delta_{22}} \left(\exp\left(-\frac{z_2}{\delta_{12}}\right) - \exp\left(-\frac{z_2}{\delta_{22}}\right) \right) dz_2 \\ &\quad \cdot \left[\int_0^{z_1} \frac{1}{\delta_{12} - \delta_{24}} \left(\exp\left(-\frac{z_3}{\delta_{12}}\right) - \exp\left(-\frac{z_3}{\delta_{24}}\right) \right) dz_3 \right]^{M-2} dz_1. \end{aligned} \quad (52)$$

The integrals in (51) and (52) are trivially evaluated, and after some mathematical manipulation, we can obtain

$$\begin{aligned} &P(c | \mathbf{x}_{s_1} = \mathbf{x}_{s_2}, h_{rs_2}) \\ &= \sum_{k_1=1}^2 \sum_{k_2=0}^{M-1} \sum_{k_3=0}^{M-1-k_2} \sum_{k_4=0}^{k_2} (-1)^{k_3+k_4} \binom{M-1}{k_2} \binom{k_2}{k_4} \\ &\quad \binom{M-1-k_2}{k_3} \frac{\delta_{12} \delta_{24} B_{14}^{M-1-k_2} B_{24}^{k_2} B_{k_1 1}}{k_3 \delta_{k_1 1} \delta_{24} + k_4 \delta_{k_1 1} \delta_{12} + \delta_{12} \delta_{24}} \\ &\quad \cdot \exp\left(-\frac{k_3 \delta_{24} + k_4 \delta_{12}}{\delta_{12} \delta_{24}} (\zeta_{m1} - \zeta_{m2})\right) \end{aligned} \quad (53)$$

and $P(c | \mathbf{x}_{s_1} \neq \mathbf{x}_{s_2}, h_{rs_2})$ which is shown on the top of the next page, where

$$B_{11} = \frac{\delta_{11}}{\delta_{11} - \delta_{21}}, \quad (55)$$

$$B_{12} = \frac{\delta_{12}}{\delta_{12} - \delta_{22}}, \quad (56)$$

$$B_{13} = \frac{\delta_{11}}{\delta_{11} - \delta_{23}}, \quad (57)$$

$$B_{14} = \frac{\delta_{12}}{\delta_{12} - \delta_{24}}, \quad (58)$$

$$B_{2p} = 1 - B_{1p}, \quad p \in \{1, 2, 3, \text{ and } 4\}. \quad (59)$$

Thus the conditional symbol-error-rate (SER) performance is

$$\begin{aligned} P_s(e | h_{rs_2}) &= 1 - \frac{M-1}{M} P(c | \mathbf{x}_{s_1} \neq \mathbf{x}_{s_2}, h_{rs_2}) \\ &\quad - \frac{1}{M} P(c | \mathbf{x}_{s_1} = \mathbf{x}_{s_2}, h_{rs_2}). \end{aligned} \quad (60)$$

We take the expectation of (60) with respect to the channel coefficients h_{rs_2} to obtain the SER performance of the optimal detector with partial CSI

$$P_s(e) = \int_{\Phi} \frac{1}{\Omega_{rs_2}} \exp\left(-\frac{z}{\Omega_{rs_2}}\right) P_s(e | h_{rs_2}) |_{|h_{rs_2}|^2=z} dz \quad (61)$$

where Φ denotes the interval $(0, \infty)$ excluding countable poles. According to [22], the BER performance of the optimal detector with partial CSI is

$$P_b(e) = \frac{M}{2(M-1)} P_s(e). \quad (62)$$

B. BER Performance Upper Bound

From (36), we know that $\rho A_r |h_{rs_2}|^2 \mathbf{x}_{s_2}$ is an interference for the detection of \mathbf{x}_{s_1} at node s_2 . If h_{rs_2} is unknown to node s_2 , the detector involves integration operation which causes the BER performance upper bound is difficult to obtain.

$$U_m = \begin{cases} \xi_{m1} = \frac{\gamma\Omega_{s_1s_2}}{N_o(1+\gamma\Omega_{s_1s_2})}|y_{s_1s_2,m}|^2 + \frac{\beta_1}{N_o}|y_{rs_2,m} - \rho A_r \sqrt{E_s}|h_{rs_2}|^2|^2; & l = m \\ \xi_{m2} = \frac{\gamma\Omega_{s_1s_2}}{N_o(1+\gamma\Omega_{s_1s_2})}|y_{s_1s_2,m}|^2 + \frac{\beta_2}{N_o}|y_{rs_2,m}|^2; & l \neq m \end{cases} \quad (43)$$

$$V_m = \begin{cases} \zeta_1 = \log \frac{1 + A_r^2|h_{rs_2}|^2(2 + \gamma(1 - \rho^2)\Omega_{rs_2})}{1 + A_r^2|h_{rs_2}|^2(2 + \gamma\Omega_{s_1r} + \gamma(1 - \rho^2)\Omega_{rs_2})}; & l = m \\ \zeta_2 = \log \frac{1 + 2A_r^2|h_{rs_2}|^2}{1 + A_r^2|h_{rs_2}|^2(2 + \gamma\Omega_{s_1r})}; & l \neq m \end{cases} \quad (44)$$

$$W_2 = \begin{cases} \delta_{21} = \beta_1 [1 + A_r^2|h_{rs_2}|^2(2 + \gamma\Omega_{s_1r} + \gamma(1 - \rho^2)\Omega_{rs_2})]; & m = l = 1 \\ \delta_{22} = \beta_1 [1 + A_r^2|h_{rs_2}|^2(2 + \gamma(1 - \rho^2)\Omega_{rs_2})]; & m \neq 1 \text{ and } m = l \\ \delta_{23} = \beta_2 [1 + A_r^2|h_{rs_2}|^2(2 + \gamma\Omega_{s_1r})]; & m = 1 \text{ and } l \neq 1 \\ \delta_{24} = \beta_2 (1 + 2A_r^2|h_{rs_2}|^2); & m \neq 1 \text{ and } m \neq l \end{cases} \quad (50)$$

$$P(c|\mathbf{x}_{s_1} \neq \mathbf{x}_{s_2}, h_{rs_2}) = \sum_{k_1=1}^2 \sum_{k_2=0}^{M-2} \sum_{k_3=0}^{M-2-k_2} \sum_{k_4=0}^{k_2} (-1)^{k_3+k_4} \binom{M-2}{k_2} \binom{M-2-k_2}{k_3} \binom{k_2}{k_4} \cdot B_{14}^{M-2-k_2} B_{24}^{k_2} B_{k_13} \cdot \exp\left(-\frac{k_3\delta_{k_1(2k_1-1)}\delta_{24} + k_4\delta_{k_1(2k_1-1)}\delta_{12} + \delta_{12}\delta_{24}}{\delta_{k_1(2k_1-1)}\delta_{12}\delta_{24}}(\zeta_{m1} - \zeta_{m2})\right) \cdot \left(\frac{\delta_{12}\delta_{24}}{\delta_{k_1(2k_1-1)}(k_3\delta_{24} + k_4\delta_{12}) + \delta_{12}\delta_{24}} - \sum_{k_5=1}^2 \frac{\delta_{k_52}\delta_{12}\delta_{24}B_{k_52}}{\delta_{k_1(2k_1-1)}(k_3\delta_{k_52}\delta_{24} + k_4\delta_{k_52}\delta_{12} + \delta_{12}\delta_{24}) + \delta_{12}\delta_{k_52}\delta_{24}}\right) \quad (54)$$

Since the interference $\rho A_r |h_{rs_2}|^2 \mathbf{x}_{s_2}$ increases the uncertainty for symbol detection and the uncertainty is measured through differential entropy, we may replace the interference with a complex Gaussian noise vector having the same differential entropy, which is denoted as \mathbf{n}_{eq} , to derive the upper bound. Thus the received signal \mathbf{y}_{rs_2} is expressed as

$$\mathbf{y}_{rs_2} = A_r h_{rs_2} (h_{s_1r} \mathbf{x}_{s_1} + \eta \mathbf{x}_{s_2} + \mathbf{n}_{s_1r} + \mathbf{n}_{s_2r})^* + \mathbf{n}_{rs_2} + \mathbf{n}_{eq} \quad (63)$$

where the covariance matrix of \mathbf{n}_{eq} is $\frac{\delta_{eq} \mathbf{x}_{s_2} \mathbf{x}_{s_2}^\dagger}{E_s}$ in which

$$\delta_{eq} = \frac{\rho A_r \Omega_{rs_2} \sqrt{E_s}}{\pi}. \quad (64)$$

Furthermore, a suboptimal receiver is obtained by approximating the received signal \mathbf{y}_{rs_2} as follows

$$\mathbf{y}_{rs_2} \approx A_r \sqrt{\Omega_{rs_2}} (h_{s_1r} \mathbf{x}_{s_1} + \eta \mathbf{x}_{s_2} + \mathbf{n}_{s_1r} + \mathbf{n}_{s_2r})^* + \mathbf{n}_{rs_2} + \mathbf{n}_{eq} \quad (65)$$

where h_{rs_2} in (63) is replaced by its square root of its variance. We can derive the performance of above-mentioned suboptimal detector which is the upper bound of our proposed optimal detector.

Assuming that $\mathbf{x}_{s_1} = \mathbf{x}_1$ and $\mathbf{x}_{s_2} = \mathbf{x}_l$, the pairwise error probability of \mathbf{x}_1 erroneously detected as \mathbf{x}_k , $k \in \{2, 3, \dots, M\}$, can be derived by using (40) where λ_{1k} is replaced by $\tilde{\lambda}_{1k}$,

$$\tilde{\lambda}_{1k} = \tilde{U}_1 - \tilde{U}_k + \tilde{V}_1 - \tilde{V}_k. \quad (66)$$

In (66), \tilde{U}_m and \tilde{V}_m , $m \in \{1, 2, \dots, M\}$, are shown on the top of the next page, where $m \in \{1, 2, \dots, M\}$,

$$\tilde{\beta}_1 = \frac{1}{1 + \delta_{eq} + A_r^2 \Omega_{rs_2} (2 + \gamma(1 - \rho^2) \Omega_{rs_2})} \quad (69)$$

$$- \frac{1}{1 + \delta_{eq} + A_r^2 \Omega_{rs_2} (2 + \gamma \Omega_{s_1r} + \gamma(1 - \rho^2) \Omega_{rs_2})},$$

TABLE I
ASYMPTOTIC ERROR BOUNDS

	$P(e \mathbf{x}_{s_1} = \mathbf{x}_{s_2})$	$P(e \mathbf{x}_{s_1} \neq \mathbf{x}_{s_2})$
Lower Bound $\rho \neq 1$	$\frac{\Lambda_1 \log \gamma}{\gamma^2}$	$\frac{\Lambda_2}{\gamma^2}$
Lower Bound $\rho = 1$	$\frac{\Lambda_3}{\gamma^2}$	$\frac{\Lambda_3}{\gamma^2}$
Upper Bound $\rho \neq 1$	$\frac{\Lambda_4}{\gamma}$	$\frac{\Lambda_5}{\gamma^2}$
Upper Bound $\rho = 1$	$\frac{\Lambda_6}{\gamma^{1.5}}$	$\frac{\Lambda_7}{\gamma^2}$

$$\tilde{\beta}_2 = \frac{1}{1 + 2A_r^2 \Omega_{rs_2}} - \frac{1}{1 + A_r^2 \Omega_{rs_2} (2 + \gamma \Omega_{s_1r})}. \quad (70)$$

Therefore, the BER performance upper bound of the optimal detector can be obtained by using (51)-(62) where W_2 is replaced by \tilde{W}_2 , shown on the top of the next page.

C. Asymptotic Error Bound Analysis

Since the derived expressions for the BER performance bounds are very complicated, we analyze the asymptotic error bounds to show the effectiveness of the proposed scheme. To simplify our analysis, we focus on the asymptotic diversity order when $M = 2$ because the diversity order is uncorrelated with the value of M [23]. Furthermore, the noise vector \mathbf{n}_{pq} is normalized such that $N_o = 1$. In Table I, we show the asymptotic error probability when $\gamma \rightarrow \infty$, where $P(e|\mathbf{x}_{s_1} = \mathbf{x}_{s_2})$ and $P(e|\mathbf{x}_{s_1} \neq \mathbf{x}_{s_2})$ denote the error probability when $\mathbf{x}_{s_1} = \mathbf{x}_{s_2}$ and $\mathbf{x}_{s_1} \neq \mathbf{x}_{s_2}$, respectively. The derivation of Λ_i , $i = 1, 2, \dots, 7$, in Table I is provided in the Appendix.

VII. SIMULATED AND THEORETICAL RESULTS

In this section, we present computer simulated and theoretical results to show the bit-error-rate (BER) performance of

$$\tilde{U}_m = \begin{cases} \tilde{\xi}_{m1} = \frac{\gamma\Omega_{s_1s_2}}{N_o(1+\gamma\Omega_{s_1s_2})}|y_{s_1s_2,m}|^2 + \frac{\tilde{\beta}_1}{N_o}|y_{rs_2,m}|^2; & l = m \\ \tilde{\xi}_{m2} = \frac{\gamma\Omega_{s_1s_2}}{N_o(1+\gamma\Omega_{s_1s_2})}|y_{s_1s_2,m}|^2 + \frac{\tilde{\beta}_2}{N_o}|y_{rs_2,m}|^2; & l \neq m \end{cases} \quad (67)$$

$$\tilde{V}_m = \begin{cases} \tilde{\zeta}_1 = \log \frac{1 + \delta_{eq} + A_r^2\Omega_{rs_2}(2 + \gamma(1 - \rho^2)\Omega_{rs_2})}{1 + \delta_{eq} + A_r^2\Omega_{rs_2}(2 + \gamma\Omega_{s_1r} + \gamma(1 - \rho^2)\Omega_{rs_2})}; & l = m \\ \tilde{\zeta}_2 = \log \frac{1 + 2A_r^2\Omega_{rs_2}}{1 + A_r^2\Omega_{rs_2}(2 + \gamma\Omega_{s_1r})}; & l \neq m \end{cases} \quad (68)$$

$$\tilde{W}_2 = \begin{cases} \tilde{\delta}_{21} = \tilde{\beta}_1 [1 + \delta_{eq} + A_r^2|h_{rs_2}|^2(2 + \gamma\Omega_{s_1r} + \gamma(1 - \rho^2)\Omega_{rs_2})]; & m = l = 1 \\ \tilde{\delta}_{22} = \tilde{\beta}_1 [1 + \delta_{eq} + A_r^2|h_{rs_2}|^2(2 + \gamma(1 - \rho^2)\Omega_{rs_2})]; & m \neq 1 \text{ and } m = l \\ \tilde{\delta}_{23} = \tilde{\beta}_2 [1 + A_r^2|h_{rs_2}|^2(2 + \gamma\Omega_{s_1r})]; & m = 1 \text{ and } l \neq 1 \\ \tilde{\delta}_{24} = \tilde{\beta}_2 (1 + 2A_r^2|h_{rs_2}|^2); & m \neq 1 \text{ and } m \neq l \end{cases} \quad (71)$$

non-coherent detection for two-way AF cooperative communications in Rayleigh fading channels. In the simulations, the fading variances are assigned by adopting a path loss model of the form $\Omega_{pq} \propto L_{pq}^{-4}$, where L_{pq} denotes the distance between nodes p and q , $p, q \in \{s_1, r, s_2\}$. The variance of Rayleigh fading coefficient from node s_1 to node s_2 is normalized such that $\Omega_{s_1s_2} = 1$. The BER performance in our plots, if not specified, is obtained by computer simulation where the expression (23) is calculated numerically.

In Fig. 2, we compare the optimal non-coherent detection of OOK (denoted as “ $M = 1$ ” in the legend) modulated one-way (denoted as “OW” in the legend) and two-way (denoted as “TW” in the legend) AF cooperative communications when $L_{s_1r} = L_{rs_2} = 0.6L_{s_1s_2}$. Throughout this paper, the transmitted power per symbol of node r for one-way cooperative communications is E_s whereas that for two-way cooperative communications is $2E_s$, i.e. $E_r = 2E_s$, for fairly comparison. This is because for one-way cooperative communication, if the node r relays the signals from nodes s_1 and s_2 with the same transmission power per symbol E_s , the total transmission power for exchanging the signals between two source nodes is $2E_s$. Thus the energy per bit, denoted as E_b , is $2E_s$.

It is found from Fig. 2 that compared with one-way scheme, OOK modulated two-way AF cooperative communications suffer performance degradation of about 2.0 dB when bit-error-rate (BER) is 10^{-3} and the channels are static, i.e. $\rho = 1$. When $\mathbf{x}_{s_2} = 0$, two-way cooperative communication scheme is reduced to one-way scheme except that the noise power of the former is twice as much as that of latter. The observed performance gap is mainly due to the fact that when $\mathbf{x}_{s_2} = \sqrt{2E_s}$, the cooperative transmission at node r includes the signal transmitted from node s_2 , which is interference for the detection of \mathbf{x}_{s_1} . When the channel is fast fading, i.e. $\rho = 0$, it is observed that two-way cooperative communication scheme provides little performance improvement over the conventional communication scheme without cooperative relaying (denoted as “No relay” in the legend). This is because when $\mathbf{x}_{s_2} = 0$, two-way scheme reduces to one-way scheme thus cooperative relaying provides additional spatial diversity gain, whereas when $\mathbf{x}_{s_2} = \sqrt{2E_s}$, the negative effect of signal transmitted from node s_2 on the detection of \mathbf{x}_{s_1} is so strong that it offsets the performance improvement when $\mathbf{x}_{s_2} = 0$.

In Fig. 2, we also compare the optimal non-coherent detection of binary FSK (denoted as “ $M = 2$ ” in the legend) modulated one-way and two-way AF cooperative communications. It is shown from Fig. 2 that both schemes perform better than OOK modulated cooperative communications. It is also found that compared with one-way cooperative communications, two-way FSK modulated cooperative communications suffer about 1.7 dB, 3.8 dB, and 4.2 dB performance degradation when the BER is 10^{-4} and $\rho = 1, 0.9$, and 0 , respectively. This is because for two-way FSK cooperative communications, the transmission of signals from node s_2 affects the detection of \mathbf{x}_{s_1} at node s_2 thus results in performance degradation.

In Fig. 3, we provide the performance comparison of optimal and suboptimal detectors for OOK and binary FSK modulated two-way AF cooperative communications. For OOK modulation, it is shown that the suboptimal detector has almost identical BER performance with the optimal detector in fast Rayleigh fading channels ($\rho = 0$). In static Rayleigh fading channels ($\rho = 1$), the suboptimal detector has about 1.3 dB performance degradation compared with the optimal detector when the BER is 10^{-3} . The observed performance gap is due to the discard of real component of $y_{rs_2,l}$ and the employment of Jensen’s inequality. From Fig. 3, it is also found that suboptimal detector for binary FSK modulated signals has a performance degradation at most 1 dB compared with optimal detector when BER is 10^{-3} and $\rho = 1, 0.9$, and 0 .

In Fig. 4, we present the theoretically derived BER performance upper and lower bounds of the BER performances obtained numerically by using (61) and (62). It is found from Fig. 4, the derived lower bound is about 1.6 dB and 0.8 dB away from the simulated BER performance when the BER is 10^{-4} and $\rho = 1$ and 0 , respectively. It is worth noting that when E_b/N_o increases, the observed gap between the lower bound and simulation results does not decrease. This is because the above-mentioned gap, from (36), is mainly due to the interference $\rho A_r |h_{rs_2}|^2 \mathbf{x}_{s_2}$ which increases with the increase of E_b/N_o . It is also noted that the derived lower bound is actually the exact BER performances of optimal detectors for FSK modulated two-way AF cooperative communications with partial channel information h_{rs_2} . From Fig. 4, the derived upper bound is about 0.6 dB and 1.5 dB away from the

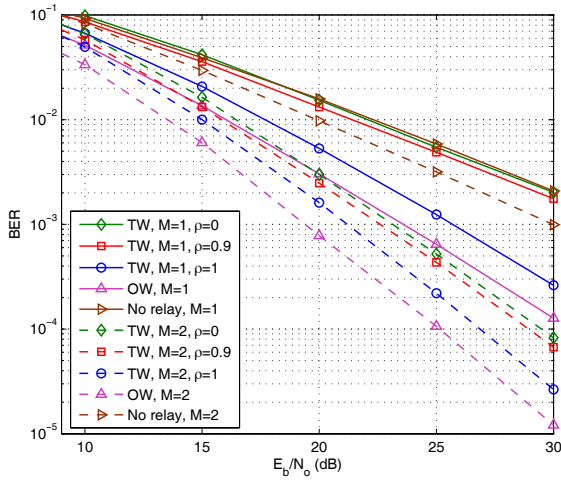


Fig. 2. BER versus E_b/N_0 ; simulated BER performance comparison of optimal detectors for one-way and two-way AF cooperative communications; $M = 1$ and 2 ; $L_{s_1r} = L_{rs_2} = 0.6L_{s_1s_2}$.

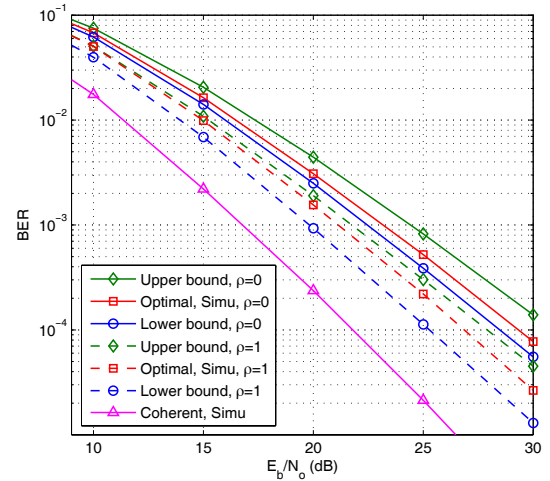


Fig. 4. BER versus E_b/N_0 ; comparison of theoretical BER performance lower bound and simulation results of optimal detector of two-way AF cooperative communications; $M = 2$; $L_{s_1r} = L_{rs_2} = 0.6L_{s_1s_2}$.

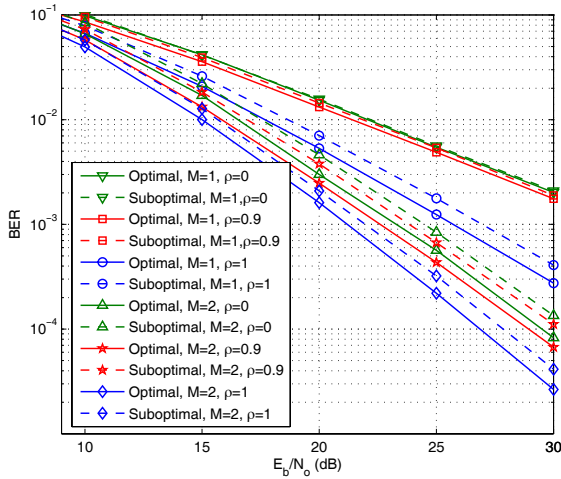


Fig. 3. BER versus E_b/N_0 ; simulated BER performance comparison of optimal and suboptimal detectors of two-way AF cooperative communications; $M = 1$ and 2 ; $L_{s_1r} = L_{rs_2} = 0.6L_{s_1s_2}$.

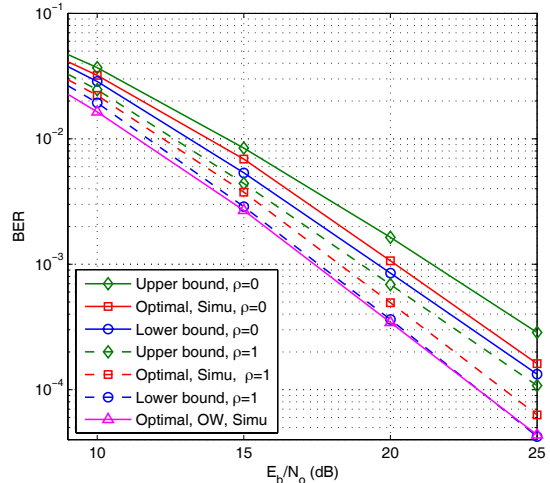


Fig. 5. BER versus E_b/N_0 ; simulated BER performance comparison of optimal and suboptimal detectors of two-way AF cooperative communications; $M = 4$; $L_{s_1r} = L_{rs_2} = 0.6L_{s_1s_2}$.

simulated BER performance when the BER is 2×10^{-4} and $\rho = 1$ and 0 , respectively.

In Fig. 4, we also present the BER performance of coherent detector for binary FSK modulated two-way AF cooperative communications (denoted as ‘‘Coherent’’ in the legend). It is shown from Fig. 4, with coherent detection, the BER performance can be significantly improved.

In Fig. 5, we compare the BER performances of 4-ary FSK modulated one-way and two-way AF cooperative communications, when $L_{s_1r} = L_{rs_2} = 0.6L_{s_1s_2}$. It is shown that compared with one-way scheme (denoted as ‘‘OW’’ in the legend), two-way scheme suffers about 0.9 dB and 3.0 dB performance degradation when the BER is 2×10^{-4} and $\rho = 1$ and 0 , respectively. The performance degradation is much less than that of binary FSK modulated AF cooperative communications. This is for the detection of \mathbf{x}_{s_1} , the signals \mathbf{x}_{s_2} transmitted from s_2 only cause interference over one

frequency and leave the other three frequencies unchanged. In Fig. 5, we also present the theoretically derived BER performance upper and lower bounds of the BER performances. It is found from Fig. 5, the derived lower bound is about 0.7 dB and 0.5 dB away from the simulated BER performance when the BER is 3×10^{-4} and $\rho = 1$ and 0 , respectively. From Fig. 5, the derived upper bound is about 1.1 dB and 1.5 dB away from the simulated BER performance when the BER is 3×10^{-4} and $\rho = 1$ and 0 , respectively.

In Fig. 6 and Fig. 7, we present BER performances of optimal detector of two-way AF cooperative communications where node r has different locations. In Fig. 6, the sum of the distances L_{s_1r} and L_{rs_2} is a constant equal to $1.2L_{s_1s_2}$. It is found from Fig. 6 that when the detection of \mathbf{x}_{s_1} is considered, the BER performance is improved if the relaying node is close to node s_1 . It is worth noting that from (8) and (23)-(24), the optimal detection scheme for the received relaying signal \mathbf{y}_{rs_2}

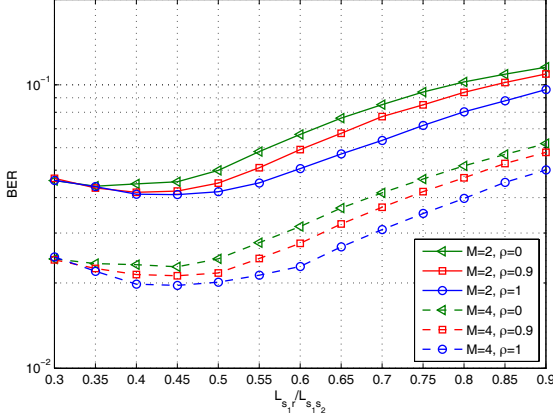


Fig. 6. BER versus L_{s1r}/L_{s1s2} ; simulated BER performance of optimal detector of two-way AF cooperative communications; $E_b/N_o = 10$ dB; $L_{s1r} + L_{rs2} = 1.2L_{s1s2}$.

is only related to the parameters E_s , E_r , N_o , ρ , Ω_{s1r} , and Ω_{rs2} . When the detection of \mathbf{y}_{rs2} is considered, the average signal-to-interference-and-noise-ratio (SINR) at node s_2 is

$$\text{SINR} = \int_0^\infty \frac{E_s \Omega_{s1r} z}{z^2 \rho^2 E_s + z(1-\rho^2) \Omega_{rs2} E_s + 2zN_o + \frac{N_o}{A_r^2}} \cdot \frac{1}{\Omega_{rs2}} \exp\left(-\frac{z}{\Omega_{rs2}}\right) dz. \quad (72)$$

When the signal-to-noise-ratio (SNR) is high, i.e. $\gamma \rightarrow \infty$, (72) is simplified as follows

$$\text{SINR} = \frac{\Omega_{s1r}}{\rho^2 \Omega_{rs2}} \mathcal{E}_1\left(\frac{1-\rho^2}{\rho^2}\right) \exp\left(\frac{1-\rho^2}{\rho^2}\right) \quad (73)$$

where $\mathcal{E}_1(\bullet)$ is the exponential integral function defined in [24, eq. (5.1.1)]. Since we employ the path loss model of $\Omega_{pq} \propto L_{pq}^{-4}$ here, when the SNR and ρ are constant, we know that the optimal relaying position is only related to L_{s1r} and L_{rs2} .

In Fig. 7, the sum of the distances L_{s1r} and L_{rs2} increases with $L_{s1r} = L_{rs2}$. It is shown from Fig. 7 that the BER performance is improved if the relaying node get close to nodes s_1 and s_2 .

VIII. CONCLUSION

In this paper, we propose optimal non-coherent detection for two-way OOK and M -ary FSK modulated AF cooperative communication schemes in fast Rayleigh fading channels. The proposed schemes provide extra spatial diversity for the communication network with single antenna transceivers. Compared with conventional one-way cooperative communications, the proposed schemes increase the system throughput at the expense of slight performance degradation. It is found from the simulation results that the proposed two-way FSK cooperative communication performs well in fast Rayleigh fading channels. Since the optimal detector for two-way AF cooperative communications involves integration operation, we propose a suboptimal detector which reduces the receiver complexity significantly at the expense of acceptable performance degradation. In this paper, we also derive the

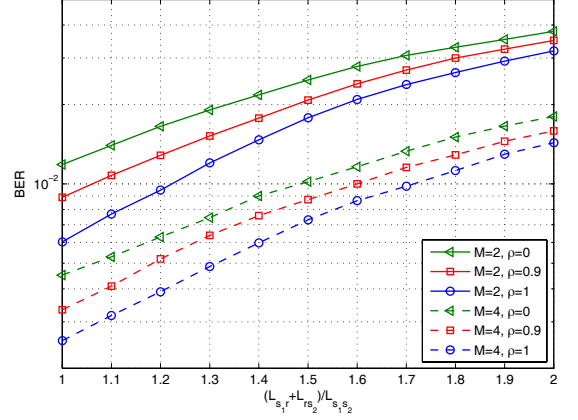


Fig. 7. BER versus $(L_{s1r} + L_{rs2})/L_{s1s2}$; simulated BER performance of optimal detector of two-way AF cooperative communications; $E_b/N_o = 15$ dB; $L_{s1r} = L_{rs2}$.

BER performance upper and lower bounds of the optimal detection for M -ary FSK modulated two-way AF cooperative communications in Rayleigh fading channels. It is found that the derived upper and lower bounds are close to the simulated BER performance.

APPENDIX

THE EXPRESSION OF $\Lambda_i, i = 1, 2, \dots, 7$

$$\Lambda_1 = \int_{\Phi} \frac{1 + 2zA_r^2}{zA_r^2 \Omega_{s1s2} \Omega_{s1r} \Omega_{rs2}} \exp\left(-\frac{z}{\Omega_{rs2}}\right) \quad (74)$$

$$\cdot \log \frac{zA_r^2 \Omega_{s1r} \Omega_{rs2} (1-\rho^2)}{(\Omega_{s1r} + \Omega_{rs2} - \Omega_{rs2} \rho^2)(1 + 2zA_r^2)} dz$$

$$\Lambda_2 = \int_{\Phi} \frac{3\Omega_{s1r} \Omega_{rs2} (1-\rho^2) + \Omega_{rs2}^2 (1-\rho^2)^2 + 3\Omega_{s1r}^2}{zA_r^2 \Omega_{s1s2} \Omega_{s1r} \Omega_{rs2} (\Omega_{s1r} + \Omega_{rs2})^2} \cdot (1 + 2zA_r^2) \exp\left(-\frac{z}{\Omega_{rs2}}\right) dz \quad (75)$$

$$\Lambda_3 = \int_{\Phi} \frac{3(1 + 2zA_r^2)}{zA_r^2 \Omega_{s1s2} \Omega_{s1r} \Omega_{rs2}} \exp\left(-\frac{z}{\Omega_{rs2}}\right) dz \quad (76)$$

$$\Lambda_4 = \int_{\Phi} \frac{(1 + 2zA_r^2)^3 \exp\left(-\frac{z}{\Omega_{rs2}}\right)}{2A_r^2 \Omega_{s1s2} (z - \Omega_{rs2})(1 + 2\Omega_{rs2} A_r^2)} \cdot \frac{1}{\Omega_{rs2}} \quad (77)$$

$$\cdot \frac{z\Omega_{s1r} + 2z\Omega_{s1r} \Omega_{rs2} A_r^2 + (1-\rho^2)(1 + 2zA_r^2) \Omega_{rs2}^2}{z\Omega_{s1r} + (1-\rho^2)\Omega_{rs2}(1 + 2\Omega_{rs2} A_r^2)} \cdot \left[\frac{\Omega_{s1r} + (1-\rho^2)\Omega_{rs2}}{\gamma(1-\rho^2)\Omega_{s1r} \Omega_{rs2}^2 A_r^2} \right]^{\frac{1+2\Omega_{rs2} A_r^2}{1+2zA_r^2}} dz$$

$$\Lambda_5 = \int_{\Phi} \left[\frac{z\Omega_{s1r}}{A_r^2 \Omega_{s1s2} \Omega_{rs2}^3 (\Omega_{s1r} + (1-\rho^2)\Omega_{rs2})^2} + \frac{z\Omega_{s1r} \Omega_{rs2} + \Omega_{rs2}^2 (\Omega_{s1r} + (1-\rho^2)\Omega_{rs2})}{zA_r^2 \Omega_{s1s2} \Omega_{s1r} \Omega_{rs2}^3 (\Omega_{s1r} + (1-\rho^2)\Omega_{rs2})} \right] \cdot (1 + 2\Omega_{rs2} A_r^2) \exp\left(-\frac{z}{\Omega_{rs2}}\right) dz \quad (78)$$

$$\Lambda_6 = \int_{\Phi} \frac{(1 + 2zA_r^2)^3}{2\pi z A_r^3 \Omega_{s1s2} \Omega_{s1r} (1 + 2A_r^2 \Omega_{rs2})^2 (z - \Omega_{rs2})} \cdot \left[\frac{(1 + 2A_r^2 \Omega_{rs2})}{\gamma^{\frac{1}{2}} \Omega_{rs2} A_r^2} \right]^{\frac{1+2\Omega_{rs2} A_r^2}{1+2zA_r^2}} \exp\left(-\frac{z}{\Omega_{rs2}}\right) dz \quad (79)$$

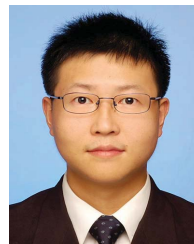
$$\Lambda_7 = \int_{\mathbb{F}} \frac{3(1 + 2A_r^2 \Omega_{r_s2})}{z A_r^2 \Omega_{s1s2} \Omega_{r_s2} \Omega_{s1r}} \exp\left(-\frac{z}{\Omega_{r_s2}}\right) dz. \quad (80)$$

REFERENCES

- [1] A. Sendonaris, E. Erkip, and B. Aazhang, "User cooperation diversity—part I: system description," *IEEE Trans. Commun.*, vol. 51, no. 11, pp. 1927–1938, Nov. 2003.
- [2] J. N. Laneman and G. W. Wornell, "Distributed space-time-coded protocols for exploiting cooperative diversity in wireless networks," *IEEE Trans. Inf. Theory*, vol. 49, no. 10, pp. 2415–2425, Oct. 2003.
- [3] J. N. Laneman, D. N. C. Tse, and G. W. Wornell, "Cooperative diversity in wireless networks: efficient protocols and outage behavior," *IEEE Trans. Inf. Theory*, vol. 50, no. 12, pp. 3062–3080, Dec. 2004.
- [4] A. E. Gamal and S. Zahedi, "Capacity of a class of relay channels with orthogonal components," *IEEE Trans. Inf. Theory*, vol. 51, no. 5, pp. 1815–1817, May 2005.
- [5] P. A. Anghel and M. Kaveh, "Exact error probabilities of a cooperative network in Rayleigh-fading environment," *IEEE Trans. Wireless Commun.*, vol. 3, no. 5, pp. 1416–1421, Sep. 2004.
- [6] R. Annavajjala, P. C. Cosman, and L. B. Milstein, "On the performance of optimum noncoherent amplify-and-forward reception for cooperative diversity," in *Proc. IEEE Military Commun. Conf.*, pp. 3280–3288, 2005.
- [7] Y. Zhu, P.-Y. Kam, and Y. Xin, "Non-coherent detection for amplify-and-forward relay systems in a Rayleigh fading environment," in *Proc. IEEE Global Telecommun. Conf.*, pp. 1658–1662, 2007.
- [8] Q. Zhao and H. Li, "Performance of differential modulation with wireless relays in Rayleigh fading channels," *IEEE Commun. Lett.*, vol. 9, no. 4, pp. 343–345, Apr. 2005.
- [9] T. Himsoon, W. Su, and K. J. R. Liu, "Differential transmission for amplify-and-forward cooperative communications," *IEEE Signal Process. Lett.*, vol. 12, no. 9, pp. 597–600, Sep. 2005.
- [10] R. Ahlswede, N. Cai, S.-Y. Li, and R. Yeung, "Network information flow," *IEEE Trans. Inf. Theory*, vol. 46, no. 4, pp. 1204–1216, July 2000.
- [11] S. Y. R. Li, R. W. Yeung, and N. Cai, "Linear network coding," *IEEE Trans. Inf. Theory*, vol. 49, no. 2, pp. 371–381, Feb. 2003.
- [12] S. Katti, H. Rahul, W. Hu, D. Katabi, M. Medard, and J. Crowcroft, "Xors in the air: practical wireless network coding," in *Proc. ACM SIGCOMM*, pp. 11–15, 2006.
- [13] P. Popovski and H. Yomo, "Wireless network coding by amplify-and-forward for bi-directional traffic flows," *IEEE Commun. Lett.*, vol. 11, no. 1, pp. 16–18, Jan. 2007.
- [14] Y. Han, S. H. Ting, C. K. Ho, and W. H. Chin, "Performance bounds for two-way amplify-and-forward relaying," *IEEE Trans. Wireless Commun.*, vol. 8, no. 1, pp. 432–439, Jan. 2009.
- [15] T. Cui, F. Gao, and C. Tellambura, "Physical layer differential network coding for two-way relay channels," in *Proc. IEEE Global Telecommun. Conf.*, pp. 1–5, 2008.
- [16] T. Cui, F. Gao, T. Ho, and A. Nallanathan, "Distributed space-time coding for two-way wireless relay networks," *IEEE Trans. Signal Process.*, vol. 57, no. 2, pp. 658–671, Feb. 2009.
- [17] R. Zhang, Y. C. Liang, C. C. Chai, and S. G. Cui, "Optimal beamforming for two-way multi-antenna relay channel with analogue network coding," *IEEE J. Sel. Areas Commun.*, vol. 27, no. 5, pp. 699–712, June 2009.
- [18] T. K. Akino, P. Popovski, and V. Tarokh, "Optimized constellations for two-way wireless relaying with physical network coding," *IEEE J. Sel. Areas Commun.*, vol. 27, no. 5, pp. 773–787, June 2009.
- [19] J. H. Sorensen, and R. Krigslund, P. Popovski, T. K. Akino, and T. Larsen, "Physical layer network coding for FSK systems," *IEEE Commun. Lett.*, vol. 13, no. 8, pp. 597–599, Aug. 2009.
- [20] M. K. Simon, *Probability Distribution Involving Gaussian Random Variables: A Handbook for Engineers and Scientists*. Springer, 2006.
- [21] M. K. Simon and M. S. Alouini, *Digital Communication over Fading Channels*, 2nd edition. Wiley, 2004.
- [22] J. G. Proakis, *Digital Communication*, 4th edition. McGraw-Hill, 2001.
- [23] A. Paulraj, R. Nabar, and D. Gore, *Introduction to Space-Time Wireless Communications*. Cambridge University Press, 2003.
- [24] M. Abramowitz and I. A. Stegun, *Handbook of Mathematical Functions with Formulas, Graphs, and Mathematical Tables*, 9th edition. Dover, 1970.



Jian Tian (S'11) received the B.Eng. (Hons.) and M.S. degrees in electrical engineering from the Chongqing University of Post and Telecommunication, Chongqing, China in 2005 and 2008, respectively. He is currently working towards his Ph.D. degree at the Shenzhen Institutes of Advanced Technology, Chinese Academy of Sciences and The Chinese University of Hong Kong. He is also with the Institute of Microelectronics and Graduate School of Chinese Academy of Sciences, Beijing. His current research interests include cooperative communications, cognitive radios, resource allocation, and signal processing in communications.



Qi Zhang received the B.Eng. (Hons.) and M.S. degrees from the University of Electronic Science and Technology of China (UESTC), Chengdu, Sichuan, China, in 1999 and 2002, respectively. He received the Ph.D. degree in Electrical and Computer Engineering from the National University of Singapore (NUS), Singapore, in 2007.

From 2007 to 2008, he was a Research Fellow in the Communications Lab, Department of Electrical and Computer Engineering, NUS. In 2008, he joined the Center for Integrated Electronics, Shenzhen Institutes of Advanced Technology, Chinese Academy of Sciences and The Chinese University of Hong Kong as an Assistant Professor and became an Associate Professor in 2010. His research interests are in cooperative communications, ultrawideband (UWB) communications, space-time coded multiple-input-multiple-output (MIMO) systems, and low-density parity-check (LDPC) codes.



Fengqi Yu was born in China and earned his Ph.D. degree in Integrated Circuits and Systems Lab (ICSL) at the University of California, Los Angeles (UCLA). In 2006, he joined the Shenzhen Institutes of Advanced Technology (SIAT), Chinese Academy of Sciences and The Chinese University of Hong Kong as a full professor and director of the Center for Integrated Electronics. Before joining SIAT, he worked at Rockwell Science (United States), Intel (United States), Teradyne (United States), Valence Semiconductor (United States), and Suzhou CAS IC Design Center (China). His R&D interests include CMOS RF integrated circuit design, CMOS sensor design, wireless sensor networks, RFID, and wireless communications.